

RESEARCH ARTICLE

Coupling of Cellular Processes and Their Coordinated Oscillations under Continuous Light in *Cyanothece* sp. ATCC 51142, a Diazotrophic Unicellular Cyanobacterium

S. Krishnakumar¹✉, Sandeep B. Gaudana¹✉, Nguyen X. Vinh⁴, Ganesh A. Viswanathan^{1,2}, Madhu Chetty⁴, Pramod P. Wangikar^{1,2,3*}

1 Department of Chemical Engineering, Indian Institute of Technology Bombay, Powai, Mumbai, India, **2** DBT Pan IIT Center for Bioenergy Indian Institute of Technology Bombay, Powai, Mumbai, India, **3** Wadhvani Research Center for Bioengineering, Indian Institute of Technology Bombay, Powai, Mumbai, India, **4** School of Information Technology, Federation University Australia, Gippsland Campus, Victoria, 3841, Australia

✉ These authors contributed equally to this work.

* wangikar@iitb.ac.in



OPEN ACCESS

Citation: Krishnakumar S, Gaudana SB, Vinh NX, Viswanathan GA, Chetty M, Wangikar PP (2015) Coupling of Cellular Processes and Their Coordinated Oscillations under Continuous Light in *Cyanothece* sp. ATCC 51142, a Diazotrophic Unicellular Cyanobacterium. PLoS ONE 10(5): e0125148. doi:10.1371/journal.pone.0125148

Academic Editor: Todd Miller, University of Wisconsin Milwaukee, UNITED STATES

Received: November 2, 2014

Accepted: March 8, 2015

Published: May 14, 2015

Copyright: © 2015 Krishnakumar et al. This is an open access article distributed under the terms of the [Creative Commons Attribution License](https://creativecommons.org/licenses/by/4.0/), which permits unrestricted use, distribution, and reproduction in any medium, provided the original author and source are credited.

Data Availability Statement: The microarray dataset was deposited to Gene Expression Omnibus (GEO) database, accession no. GSE65429.

Funding: The work was partially funded by an Australia-India strategic research (AISRF) grant to PPW and MC. The grant to the Indian side was provided by Department of Biotechnology, Ministry of Science and Technology, Government of India, grant number: BT/Indo-Aus/04/04/2009. The funders had no role in study design, data collection and analysis, decision to publish, or preparation of the manuscript.

Abstract

Unicellular diazotrophic cyanobacteria such as *Cyanothece* sp. ATCC 51142 (henceforth *Cyanothece*), temporally separate the oxygen sensitive nitrogen fixation from oxygen evolving photosynthesis not only under diurnal cycles (LD) but also in continuous light (LL). However, recent reports demonstrate that the oscillations in LL occur with a shorter cycle time of ~11 h. We find that indeed, majority of the genes oscillate in LL with this cycle time. Genes that are upregulated at a particular time of day under diurnal cycle also get upregulated at an equivalent metabolic phase under LL suggesting tight coupling of various cellular events with each other and with the cell's metabolic status. A number of metabolic processes get upregulated in a coordinated fashion during the respiratory phase under LL including glycogen degradation, glycolysis, oxidative pentose phosphate pathway, and tricarboxylic acid cycle. These precede nitrogen fixation apparently to ensure sufficient energy and anoxic environment needed for the nitrogenase enzyme. Photosynthetic phase sees upregulation of photosystem II, carbonate transport, carbon concentrating mechanism, RuBisCO, glycogen synthesis and light harvesting antenna pigment biosynthesis. In *Synechococcus elongates* PCC 7942, a non-nitrogen fixing cyanobacteria, expression of a relatively smaller fraction of genes oscillates under LL condition with the major periodicity being 24 h. In contrast, the entire cellular machinery of *Cyanothece* orchestrates coordinated oscillation in anticipation of the ensuing metabolic phase in both LD and LL. These results may have important implications in understanding the timing of various cellular events and in engineering cyanobacteria for biofuel production.

Competing Interests: The authors have declared that no competing interests exist.

Introduction

Cyanobacteria are being keenly explored for carbon dioxide capture and conversion to biomass and biofuels [1,2]. Cyanobacteria, a group of prokaryotes, perform oxygenic photosynthesis and are responsible for a significant fraction of primary production on earth. The fixed organic carbon can be utilized directly or processed into high value commodities including biofuels. Some cyanobacteria also fix nitrogen, contribute significantly to the global nitrogen cycle [3] and may play an important role in the nitrogenase mediated production of hydrogen [4]. The nitrogenase enzyme complex is sensitive to molecular oxygen and therefore, cyanobacteria are remarkable for their ability to perform oxygenic photosynthesis and nitrogen fixation within a single cell. Unicellular nitrogen fixing cyanobacteria such as *Cyanothece* sp. temporally separate these seemingly incompatible metabolic pathways [5,6] while heterocyst forming cyanobacteria such as *Nostoc* sp. employ spatial separation to protect the nitrogenase enzyme from molecular oxygen [7].

Several studies have demonstrated that the global gene expression in cyanobacteria is under the control of an internal circadian clock that pre-empts the need to sense light or time of the day in real time [8]. This provides an advantage to the cells as they are able to get ready for the ensuing day or night. While the clock components and the mechanism of circadian control are most well enumerated in a model cyanobacterium *Synechococcus elongatus* PCC 7942 (henceforth *Synechococcus* 7942) [9], all sequenced cyanobacteria contain majority of the key clock components [10]. The circadian control is exerted through a core molecular clock, input pathways that sense environmental cues and output pathways that transmit signal to the functional genes. The core clock is comprised of three proteins: KaiA, KaiB and KaiC with KaiC as the central oscillator that undergoes phosphorylation-dephosphorylation cycles of 24 h period [11,12]. The core clock receives cues from the environment through the components of input pathway such as CikA and RpaA and passes on signal to the output pathway components such as PatB, NtcA and SasA [13]. The input to the clock is most likely received through physiological parameters such as intracellular redox state [14] or the ATP to ADP ratio [15,16].

In recent years, *Cyanothece* sp. ATCC 51142 (henceforth *Cyanothece* 51142), a unicellular diazotroph, is being explored as another model organism for studies on the circadian rhythm [17–20]. *Cyanothece* 51142 is reported to produce highest amount of hydrogen amongst all the studied wild type cyanobacterial strains. Importantly, the strain shows robust oscillations in metabolism even under continuous light. The oscillations can be observed as rhythmic buildup and depletion of intracellular glycogen as well as in real time with exhaust gas CO₂ and O₂ analysis [21,22]. This enables sampling of the culture under specific metabolic phases and subsequent correlation of the gene expression results with the physiology of the organism. On the contrary, *Synechococcus elongatus* PCC 7942 (henceforth *Synechococcus* 7942) does not show any appreciable oscillations in metabolism under LL despite significant and observable oscillations in gene expression [23,24].

In a previous study, the rhythmicity of gene expression of *Cyanothece* 51142 under LL may not have been fully captured possibly because the study was limited to the first 24 h of LL [25]. We have recently shown that although the culture shows a cycle time of ~11 h under LL, it takes ~20 h for the new rhythm to set in after switching to LL [18]. To the best of our knowledge, the present study is the first one that correlates the oscillations in global gene expression to those in metabolism in cyanobacteria in continuous light. We observe that genes associated with a large number of diverse cellular functions including but not restricted to central metabolism and circadian rhythm oscillate with a period of ~11 h under LL. Starting with a formal treatment for periodicity analysis, we investigate into the temporal juxtaposition of the various cellular events in a shortened “day” of ~11 h in *Cyanothece* 51142. Our analysis points to an interesting possibility that the metabolic state of the cell drives the “circadian rhythm” rather than the opposite.

Materials and Methods

Culture growth

Axenic cultures of *Cyanothece* 51142 were cultivated in ASP2 medium without nitrate [6] in air-sparged and stirred bioreactor with external illumination of 230 μmol photons, as described earlier [18]. The organism was grown under highly turbulent conditions, equivalent to 30000 Reynolds number, to simulate flashing light effect [22]. The culture was entrained under light/dark cycles (12 h /12 h) (LD) for 4 days and then released into continuous light (LL). The growth of the organism was monitored by measuring the optical density at 730 nm (OD_{730nm}).

RNA extraction and microarray

Samples were drawn to extract RNA for microarray analysis such that the product of volume and OD_{730nm} was 50.0. The same RNA samples were also used for Real-time PCR analysis for validation of microarray results [18]. Nine samples were drawn from two consecutive cycles under LL (S1 Fig). Microarray analysis was performed at Mogene (St. Louis, USA) as described earlier [19]. Briefly, total RNA from individual samples and an equi-molar mixture of all samples as control were labeled with Cy3 and Cy5, respectively. Unbound dyes were removed using RNA clean kit (Zymo Research, Irvine, CA). Two biological replicates, two technical replicates and a dye swap were analyzed for each sample from individual time points. The microarray dataset submitted to Gene Expression Omnibus (GEO) database, accession no. GSE65429.

Models for identifying gene periodicity

We employ two complementary models to detect gene periodicity. First, we fit a single sinusoidal component to expression profile of each gene [26]. This model can be used for exploratory investigation into major periodicities present in the data. Subsequently, we employ a more rigorous statistical test for periodicity based on the Fourier score [27]. This test requires that a suspected periodicity T (or a set of periodicities) be specified. To ensure statistical rigor, we select genes that satisfy both conditions.

Sinusoidal model for Periodicity

As in [26], the gene expression dynamics can be modeled by employing a sinusoidal component together with a linear term (Eq (1)).

$$g(t) = a + bt + A \sin(2\pi Tt + \phi) + error(t) \quad (1)$$

where (A, T, φ) are the amplitude, period and phase of the sinusoidal component, while the (a + b t) term reflects the linear trend of expression level and may account for temporal drift in the data.

Let (t_i, g_{obs}(t_i)), i = 1 . . n be the actual (time, observed measurement) pairs for the n time points. We first remove the linear trend via linear regression, with a and b estimated as:

$$a = \frac{\sum g_{obs}(t_i) - b \sum t_i}{N}, \quad (2)$$

$$b = \frac{N \sum g_{obs}(t_i) t_i - \sum g_{obs}(t_i) \sum t_i}{N \sum t_i^2 - (\sum t_i)^2}$$

Thus, the observed rhythmic component of the signal can be obtained as follows:

$$r_{obs}(t_i) = g_{obs}(t_i) - a - bt_i, \quad i = 1 \dots n \quad (3)$$

The rhythmic component parameters are obtained by minimizing the following Squared Residual Error (SRE):

$$SRE = \sum_{i=1}^N [r_{obs}(t_i) - A \sin(2\pi T t_i + \phi)]^2 \tag{4}$$

Minimizing the SRE in (4) is a non-linear, non-convex optimization problem in the parameter set $\{A, T, \phi\}$. Thus, local optimization procedures will need a good initial estimate to converge to a good solution. We solve this optimization problem as follows. First, we initialize the period T from 1h to 36h in step of 0.5h, while the other parameters are initialized as $A = \max_{i=1..n} r_{obs}(t_i)$, $\phi = 0$. Matlab's lsqcurvefit function is employed to minimize the error function from the initial guess. The period that results in the smallest residue is taken as the optimal period. An illustration for the model fitting process is given in Fig 1A. To assess the goodness-of-fit, we compute the residue percentage energy, defined as

$$RPE = \frac{\sum_i [r_{obs}(t_i) - A \sin(2\pi T t_i + \phi)]^2}{\sum_i [A \sin(2\pi T t_i + \phi)]^2} \tag{5}$$

We deem RPE values of less than 25% to be a good fit.

Fourier Score for Periodicity

When employing the sinusoidal model, there is always a possibility of missing those genes which have irregular patterns and whose oscillatory behaviour is significantly non-sinusoidal. To address this, we complement the sinusoidal model with a statistical test for periodicity, as detailed next. In order to test for statistical significance of periodicity in gene expression profiles, we employ the Fourier score, defined as:

$$F = \sqrt{\left(\sum_{i=1}^n \sin \omega t_i \cdot g_{obs}(t_i)\right)^2 + \left(\sum_{i=1}^n \cos \omega t_i \cdot g_{obs}(t_i)\right)^2} \tag{6}$$

Where $\omega = 2\pi / T$.

In a recent work [27], the Fourier score coupled with a permutation test was found to be effective for identifying gene behaving in a cyclic manner. Thus, here we also employ a permutation test with 10,000 permutations generated. The *p*-value for each gene is calculated based on the fraction of random profiles that has a Fourier score equal or higher than that of the gene being studied. It is to be noted that for this test, the period T must be provided a priori. We use the sinusoidal model to identify the periods. Since the number of tests being performed is large, we employ the false discovery rate (FDR) controlling procedure [28] to set a global threshold for *p*-value. In particular, the *p*-value of the genes are sorted in increasing order $p_1 \leq p_2 \leq \dots$. Fix a false discovery rate q^* , and identify *k* as the largest *i* for which $p_i \leq q^* i/m$, where *m* is the number of tests, i.e. number of genes in this case. Then, all genes corresponding top₁, p₂, ... , p_k are designated as periodic genes with period T.

Results and Discussion

Gene expression under constant light

Roughly 30% of *Cyanotheca* genes oscillate under diurnal cycles [19]. Further, *Cyanotheca* culture oscillates between photosynthesis and respiration with a cycle time of ~11 h under LL

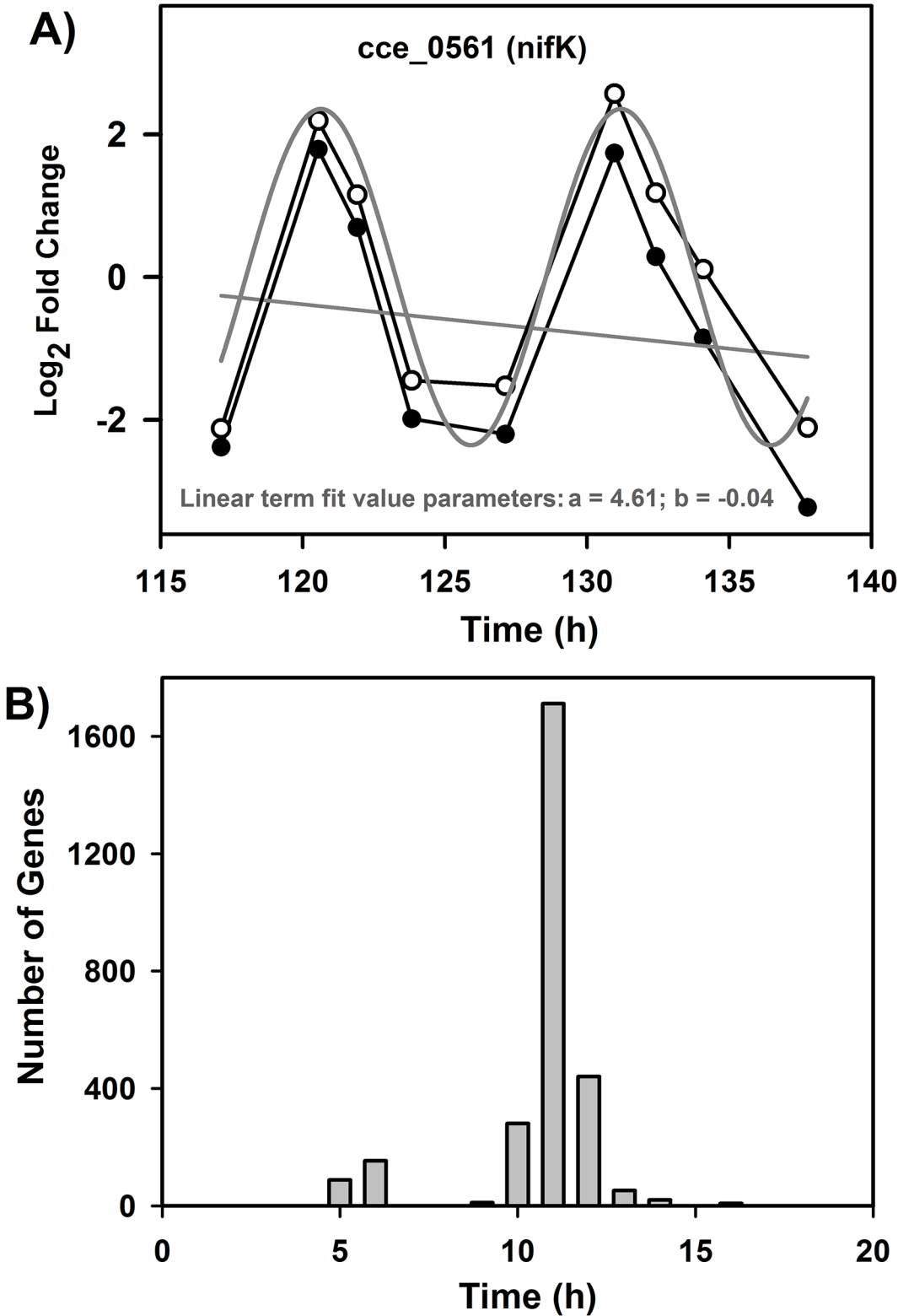


Fig 1. Sinusoidal model fitting to cyclic genes and estimation of model parameters. A: Results shown for *nifK* gene (*cce_0561*) as a representative under continuous light with the observed expression profile (●), linear term of the model (grey straight line, $a + b \cdot t$ from Eq (1)), data points after subtracting the linear term (○) and sinusoidal fit (grey sinusoidal curve). B: Histogram showing periodicity of oscillation for $n = 2152$ genes, deemed to be cyclic by sinusoidal model with a cut-off of 25 percent residual percent energy as a measure of goodness of fit.

doi:10.1371/journal.pone.0125148.g001

[17,18]. A select *Cyanothece* genes have also been shown to oscillate under LL [18]. Thus, it was of interest to determine if this was a genome-wide phenomenon and if the oscillations included cellular events other than metabolism. To that end, we obtained genome-wide gene expression time-course with DNA microarray during the photosynthetic, respiratory and transition phases of the culture under LL (S1 Fig). After a four-day entrainment, the culture takes ~20 h to settle into rhythmic oscillations. Thus, a total of 9 samples were collected from LL_{21.1} to LL_{41.75}, covering two complete cycles of metabolic oscillations. Sample numbers 1, 5 and 9 are at the transition from photosynthetic to respiratory metabolism while samples 3 and 7 mark the reverse transition. Samples 2 and 6 are at the peak of respiration while samples 3 and 7 are at the peak of photosynthesis. Of the 5251 genes, 2984 genes showed > 2-fold change across the samples while 4755 genes satisfied a less stringent 1.5-fold change filter. When sorted by the average of raw intensity in the time course, the top 200 highly expressed ORFs comprised of components of ribosome, photosystems I and II, the nitrogenase complex, phyco-cyanin, allophycocyanin, cytochrome b6-f complex, ATP synthase, and hemeoxygenase (S1 Table). This list also contained over 100 hypothetical proteins suggesting that the unannotated genes may be involved in key cellular processes. Notably, majority of the top 200 highly expressed genes show > 1.5 fold change during the experiment. Highly expressed genes are also of interest for development of expression systems, promoters and ribosome binding sites for efficient heterologous protein expression.

Detection of cycling genes and their periodicities

We employ a two-stage procedure comprising a sinusoidal model [26,29] and Fourier score [27,30] to detect cycling genes and to estimate periodicity of cycling (*T*) as detailed in the materials and methods section. We first select 4755 of *Cyanothece* genes that satisfy 1.5-fold change threshold (Table 1) and delineate the linear trend or drift component from data for each gene (Fig 1A). A sinusoidal model is then fit and the residue percentage energy estimated as a measure of goodness of fit. A histogram of the estimated *T* values shows that majority of genes

Table 1. Comparison of cyclic genes between *Cyanothece* 51142 and *Synechococcus* 7942.

	<i>Cyanothece</i> 51142		<i>Synechococcus</i> 7942
	Present Study	Data from [19]	Data from [32]
Light Regime ^a	LL	LD	LL
Number of genes	5251	4666	2662
Genes that pass the 1.5 fold filter	4755	1863	1218
Periodicity (T)	11±1	24±1	24±1
Model 1 predicted cyclic genes	2710	1024	636
Model 1 predicted cyclic genes satisfying T and RPE ^b (25%)	2152	540	300
Model 2 predicted cyclic Genes	1705	1673	972
Genes that satisfy both Models	1202	540	300
Genes that satisfy either Models	2655	1673	972
Genes that satisfy none of the Models	1453	1133	672
Genes that satisfy Model 1 only	950	0	0
Genes that satisfy Model 2 only	503	1133	672

Two models, Sinusoidal model (Model 1) and Fourier score based model (Model 2) were used to test cyclic behavior of a given gene.

^aLD: light dark cycles of 12 h each, LL: Continuous light.

^bResidual Percentage Error

doi:10.1371/journal.pone.0125148.t001

cycle with a T of ~ 11 h (Fig 1B). T value of 11 ± 1 h is observed for 2710 genes of which 2152 genes show a satisfactory goodness of fit (Table 1). According to the Nyquist-Shannon sampling theorem [31], the minimum T value that can be accurately estimated with the current data is 5.6 h. Thus, the data supports the estimation of T of ~ 11 h but not of 5 h as seen in the smaller peak in the histogram (Fig 1B). To further verify the main frequency of $T \sim 11$ h, we provide the scatter plots for $x(t)$ vs. $x(t+11$ h) and $x(t)$ vs. $x(t+5.5$ h), where $x(t)$ is the expression value of a gene at time t (Fig 2). There exists a strong positive correlation for $x(t)$ vs. $x(t+11$ h) as expected, while the plot for $x(t)$ vs. $x(t+5.5$ h) exhibits a strong negative correlation.

Having identified the major periodicity within the data being around 11 h, we next employ the statistical test based on Fourier score, as detailed in materials and methods section, to filter out those genes with significant periodicity in the vicinity of 11 h. In particular, for each gene, we perform 5 tests, with the period T fixed at 10 h, 10.5 h, 11 h, 11.5 h and 12 h, and record the smallest p -value. Next, the false discovery rate controlling procedure was carried out, with q^* fixed at 5%. At this threshold, we identify 1705 genes as having a significant near 11 h periodicity. In total, using both procedures, we identify 1202 genes satisfying both conditions. We deem this set of genes as having periodic expression profile for further analysis. A list of genes and gene expression data has been provided for genes that satisfy the 1.5-fold change threshold, the sinusoidal model, the statistical model or both models has been provided in S2 Table–S4 Table.

We performed analysis of cyclic genes with reported gene expression data for *Cyanotheca* under diurnal cycles [19] and *Synechococcus* 7942 under constant light [32] (Table 1). Firstly,

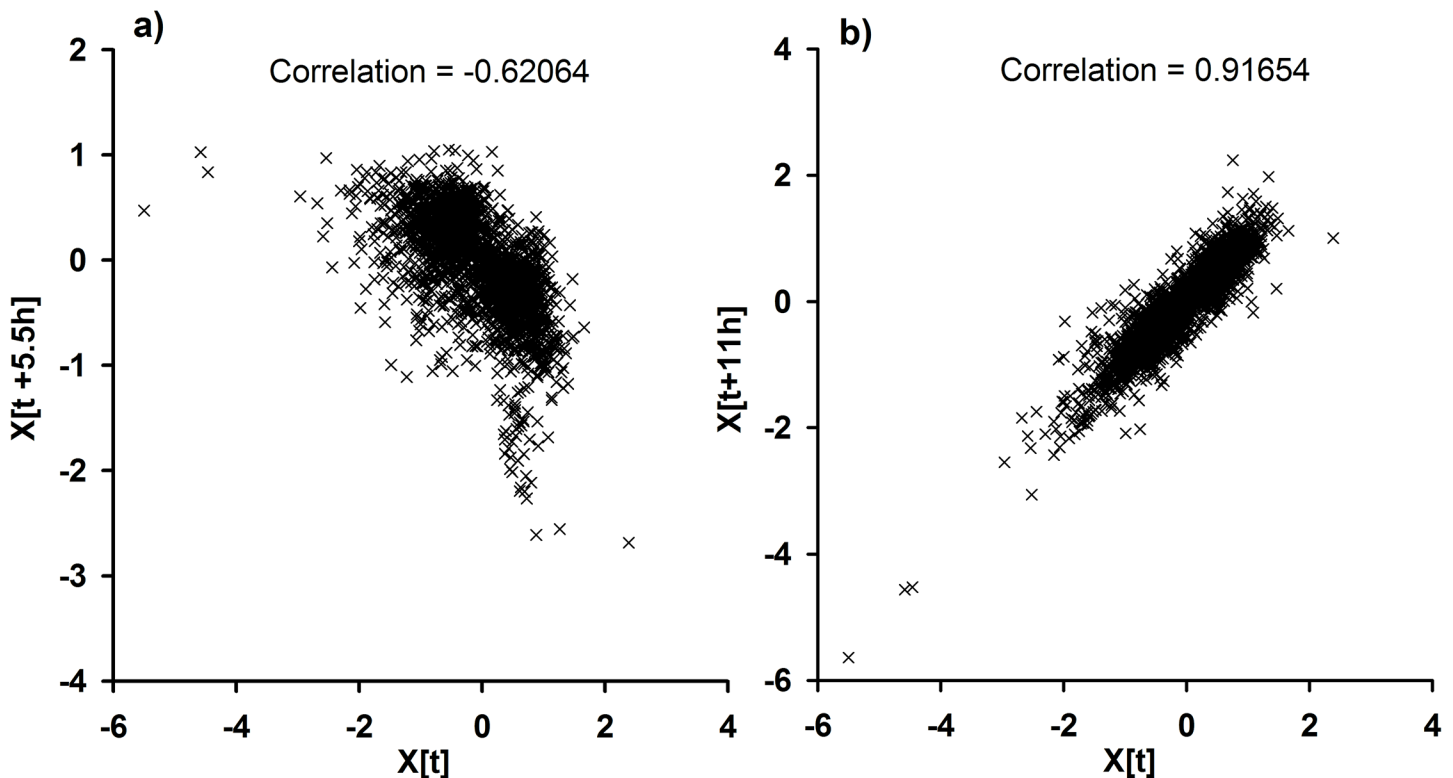


Fig 2. Scatter plot to demonstrate 11 h as the predominant periodicity among the cyclic genes. A scatter plot for 2152 genes that show satisfactory goodness of fit in the sinusoidal model with a randomly selected time point of $t_{1,21.92h}$ as x-axis and its respective $t+5.5h$ ($t_{1,27.13h}$) or $t+11h$ ($t_{1,32.42h}$) as the y-axis. A: Scatter plot showing a negative correlation between the gene expression at t and $t+ 5.5$ h. B: Scatter plot showing a positive correlation between the gene expression at t and $t+11$ h.

doi:10.1371/journal.pone.0125148.g002

these studies report a relatively smaller fraction of genes that pass the 1.5-fold change threshold. We believe that this may be partially due to the differences in culturing conditions where we minimize light limitation by creating a simulated flashing light effect by growing the culture in turbulent regime [22,33]. In both the studies, the major periodicity element was of 24 h. Interestingly, only a small fraction of genes fit the sinusoidal model although a larger number of genes pass the Fourier score criteria.

Equivalence between time of day in diurnal cycles and metabolic phase in continuous light

The net rates of CO₂ uptake and O₂ evolution (as estimated from exhaust gas analysis) allow us to monitor the metabolic phase of the culture in real time. Under diurnal cycles, the culture is observed in three broad categories of metabolic phases: (i) photosynthetic phase from dawn till ~1 h before dusk, (ii) respiratory phase from ~1 h pre-dusk to ~4 h into dark and (iii) maintenance phase with low respiration rates for the remaining ~8 h of dark cycle (S1 Fig). Under LL, both the photosynthetic and respiratory phases are shorter by 2–3 h each while the maintenance phase is absent thereby resulting in an 11 h cycle time. First, it was of interest to ascertain if the consecutive metabolic cycles under LL result in reproducible cycling of gene expression. A heatmap of the genes, upon hierarchical clustering and with correlation as a metric, shows peaking times for groups of genes (Fig 3). The genes that peak at a particular time during the first metabolic cycle also peak at an equivalent phase in the second cycle. Next, it was of interest to compare the peaking behaviour of genes under LL and LD and correlate this with the respective metabolic cycling. To that end, we selected genes that pass the 1.5-fold change threshold under diurnal cycles [19] and continuous light (this study) and subjected to K-means clustering with K = 40 clusters and correlation as a metric (S5 Table). Examination of representative clusters reveals that genes that peak at dawn also peak at the beginning of the photosynthetic phase under LL (i.e., data points 3 and 7) (e.g., Fig 4A–4I) while the mid-day peaking genes peak during late photosynthetic phase under LL (i.e., data points 4 and 8) (e.g., Fig 4E). By the same token, genes that peak at dusk peak at the beginning of respiration phase under LL (i.e. data points 1, 5 and 9) (e.g., Figs 5A–5C and 6B and 6D). Fig 5D and 5F are examples of genes that peak during early dark or mid-respiration under LL (points 2 and 6). This clearly establishes the metabolic and gene expression equivalence between the various phases of the 11 h cycle under LL with the time of day under LD. We then use the Biological Networks Gene Ontology tool (BiNGO) to systematically check for overrepresentation of Gene Ontology (GO) terms in the 40 clusters [34]. We find that a number of clusters are enriched in Functional category or GO terms (Table 2). Some of the enriched functions included the expected categories of photosystem I, nitrogen fixation and proton-transporting ATP synthase complex.

Oscillation between carbon and nitrogen uptake

Cyanothece 51142 oscillates between carbon uptake during light phase and nitrogen uptake during dark phase under diurnal cycles [4,17,35]. This arrangement suits the organism as the two processes are incompatible. We and others have reported oscillation between photosynthesis and respiration for this strain even under continuous light (S1 Fig). Photosynthesis is accompanied by upregulation of genes associated with photosynthesis, carbon uptake and glycogen synthesis (Fig 4). On the contrary, the respiration phase is characterized by upregulation of genes involved in glycogen degradation, TCA cycle, oxidative pentose phosphate pathway and nitrogen fixation (Fig 5). We believe that these oscillations serve the purpose of maintaining a healthy Carbon-Nitrogen (C/N) ratio within the cells under continuous light. Since the nitrogen fixation and photosynthesis (or carbon fixation) processes are not

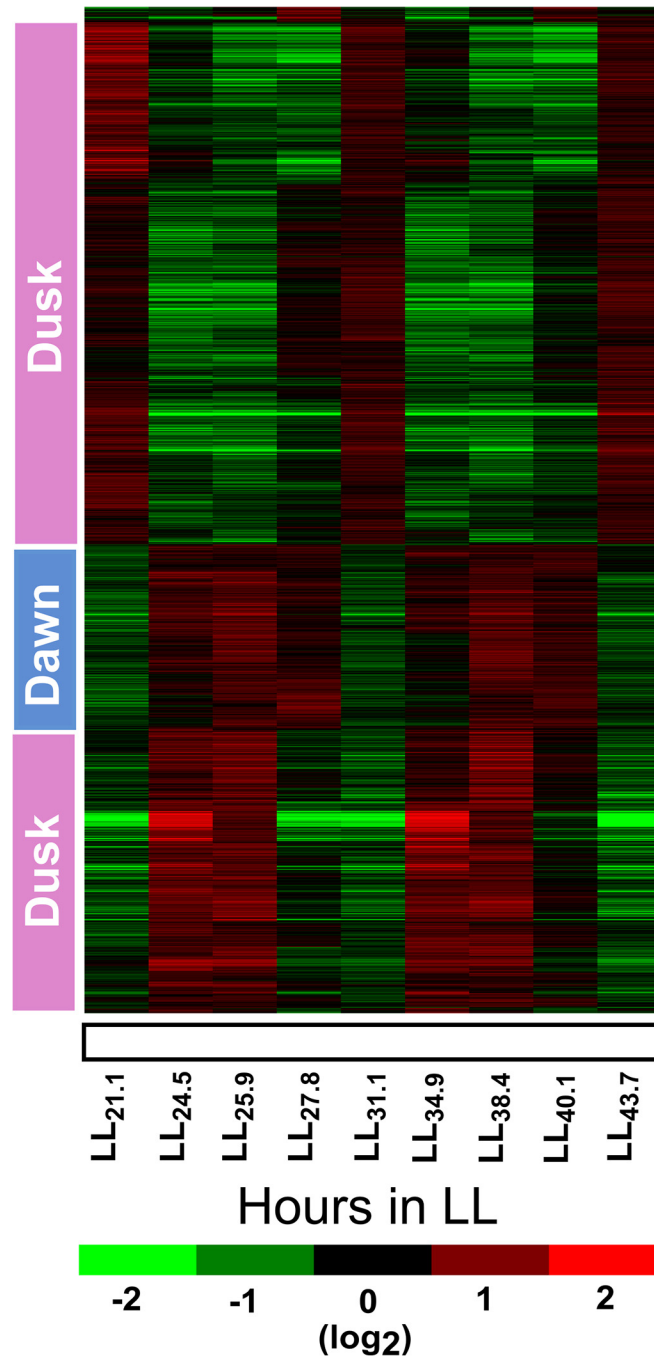


Fig 3. Heat map and hierarchical clustering of cyclic genes. Heat map was generated by performing hierarchical clustering for 1202 genes, which show 11h periodicity in oscillations and satisfy both Sinusoidal and Fourier Transform based models. Genes that peak under photosynthesis or respiration based metabolism are marked notionally as dawn peaking and dusk peaking, respectively. Normalized gene expression value, \log_2 (fold change) is plotted as per the scale bar shown below the x-axis.

doi:10.1371/journal.pone.0125148.g003

compatible, lack of oscillations may lead to continuous carbon fixation and nitrogen starvation or vice versa.

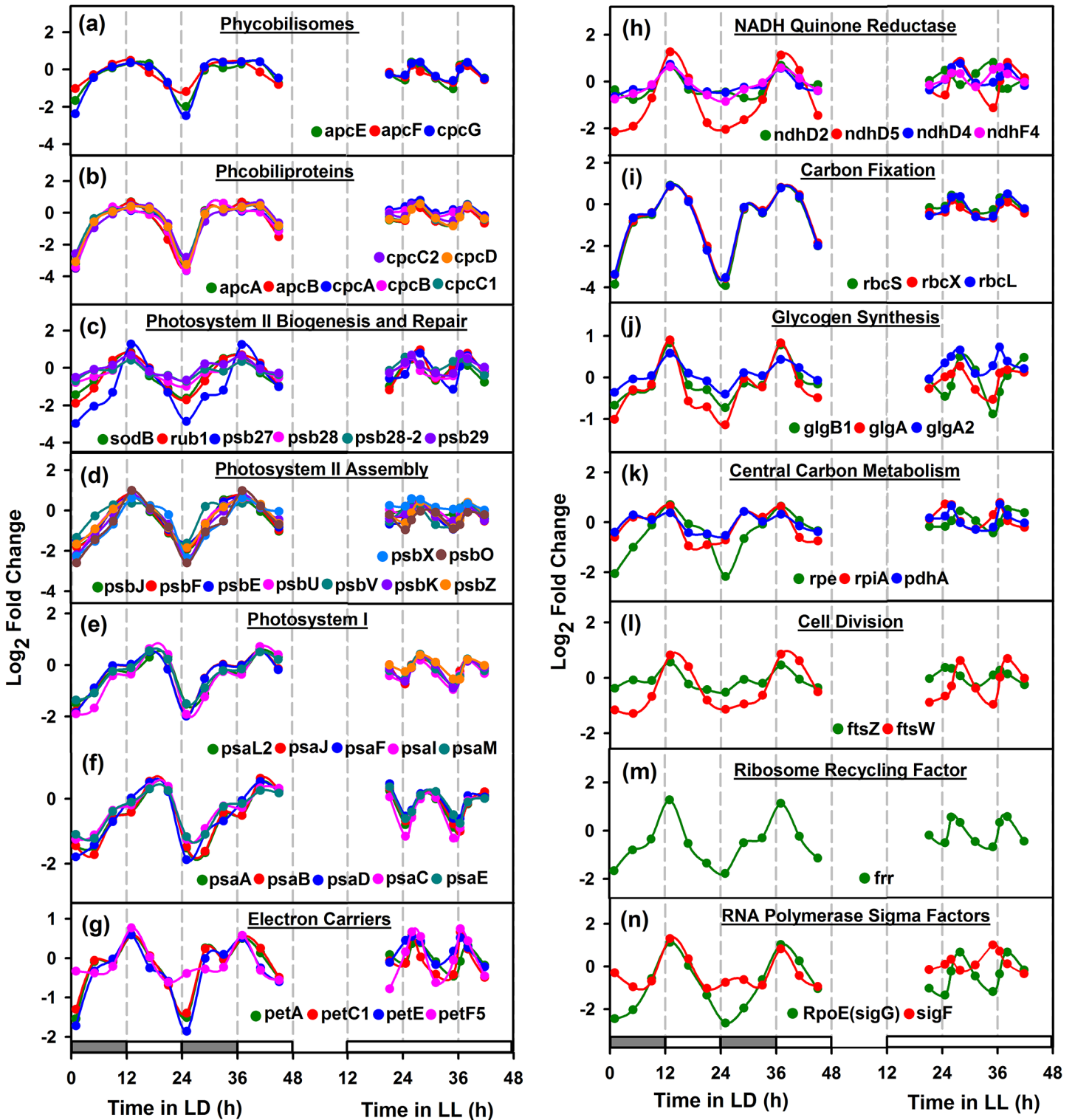


Fig 4. Day peaking oscillatory genes of *Cyanotheca* 51142. Genes were selected based on 1.5-fold change cutoff and clustered using the gene expression data under continuous light (LL) (present study) and light/dark (LD) condition [19]. Panels (a) and (b) show the essential genes that are involved in the organization of Phycobilisomes and Phycobiliproteins; panels (c) and (d) show the genes that participate in biogenesis, repair and assembly of Photosystem II. Panels (e) and (f) refer to the genes that are involved in functioning of Photosystem I, peaking during the mid-day or mid of the photosynthetic phase. Panel (g)-(h) represent genes that participate in the electron transport chain and panels (i)-(k) represent the genes that play an important role in carbon fixation, glycogen synthesis and central carbon metabolism. Panels (l)-(n) show the genes that are involved in cell division, ribosome recycling, RNA

polymerase sigma factor, where all up-regulate at dawn or during the onset or middle of the photosynthetic phase to support cell growth and maintenance. Grey and White filled and continuously white filled boxes in the X-axis, indicate the culture growth conditions of LD and LL, respectively.

doi:10.1371/journal.pone.0125148.g004

Genes peaking during photosynthetic phase

[Fig 4](#) shows peaking behavior of representative genes that peak during the photosynthetic phase under LL. Photosystems (PS) I and II, accessory proteins and pigments, RuBisCO, among others fall in this category. Phycobilisomes or the light harvesting antennae of cyanobacteria are comprised of phycocyanin, allophycocyanin and other accessory proteins. Components of phycobilisomes ([Fig 4A and 4B](#)), PS II ([Fig 4C and 4D](#)), RuBisCO subunits ([Fig 4I](#)) get upregulated during early photosynthetic phase (time points 3 and 7) under LL. Components of PS I, on the other hand, exhibit delayed response and peak during mid-day under LD and mid-photosynthetic phase (time points 4 and 8) under LL ([Fig 4E and 4F](#)). [Fig 4](#) also includes examples of genes that are dawn peaking under LD but peak at mid-photosynthetic phase under LL ([Fig 4J and 4N](#)). For instance, the oscillations in glycogen synthesis genes ([Fig 4I](#)) show the aforementioned pattern of oscillations. The expression of glycogen synthesis genes is possibly dependent on the intracellular glycogen concentration, which also oscillates at ~11h frequency under LL, however with reduced amplitudes[18]. So, possibly in absence of external constraints of light/dark cycles, the glycogen synthesis genes expression is driven solely by the depletion of intracellular glycogen content.

Carbon concentrating mechanism

Many cyanobacteria have devised a carbon concentrating mechanism (CCM) through which the process of carbon fixation occurs within the proteinaceous micro-compartments called carboxysomes. Carboxysomes encapsulate the principle carboxylating enzyme ribulose biphosphate carboxylase/oxygenase (RuBisCO) for efficient enzymatic activity of this enzyme mediated by elevated CO₂ concentration around it. The gene expression pattern of the CCM genes and that of the RuBisCO precedes the beginning of the photosynthesis phase as well as the expression of the photosystem genes (Figs [4I](#) and [7A](#)). This should be for facilitating the assembly of the carboxysome and the encapsulation of RubisCO to ensure that the carbon fixation machinery is ready when the photosynthesis begins. Interestingly, in *Cyanothece* 51142, the size of carboxysomes is predicted to be around 250–600 nm [36], which is significantly larger than those in other cyanobacteria which ranges around 100 to 200 nm [37,38]. Intriguingly, the expression patterns of many CCM genes such as *ccmM*, *ccmL*, *ccmK1* and *ccmK2* coincide with the expression of *nif* genes, suggesting the possibility of the micro-compartmentalisation of nitrogenase as a mechanism for its protection from oxygenic inactivation. Co-localization studies of nitrogenase with the carboxysome shell proteins in *Cyanothece* 51142 should yield a better explanation on oxygen protection mechanism in this organism, especially during growth under constant light.

Housekeeping Genes

Housekeeping genes are genes involved in basic cellular functions and are understood to be constitutively expressed. However several genes conventionally believed as housekeeping have been observed to show an oscillating pattern of expression in cyanobacteria [8] and it is hence deemed appropriate to not go with a priori determination of constitutive genes while analysing the transcriptome datasets in cyanobacteria [39]. Under the present study we observe an oscillating gene expression of *gap* ([Fig 6F](#)), a gene annotated as housekeeping, similar to the peaking of sigma factors. Other designated housekeeping genes ([S2 Fig](#)) show an expression pattern

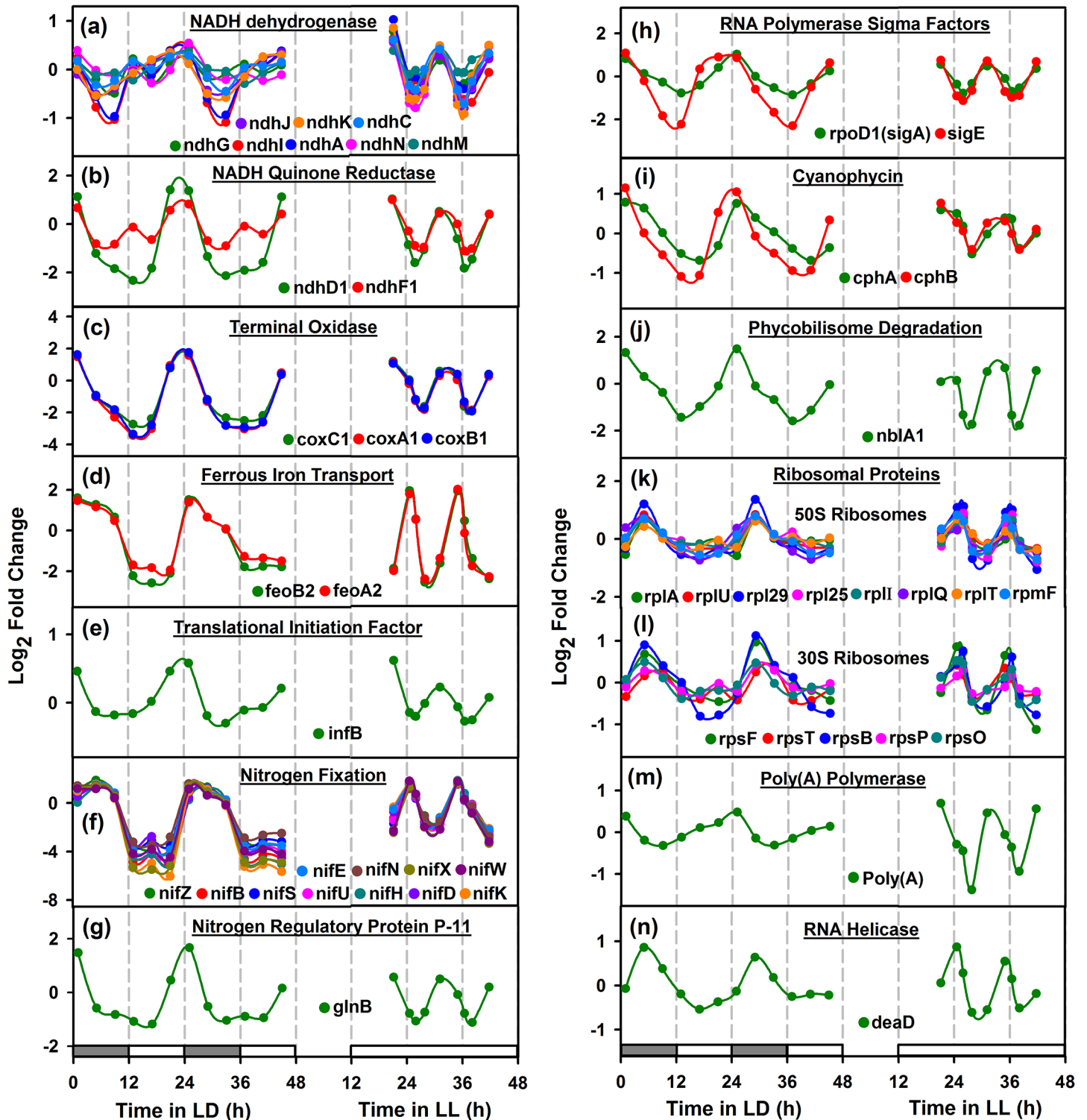


Fig 5. Night peaking oscillatory genes of *Cyanothecce* 51142. Panels (a)-(c) show the genes that are involved in NADH dehydrogenase, NADH quinone reductase and terminal oxidase of oxidative phosphorylation pathway, peaking at dusk or prior to the onset of respiration phase. Panels (d)-(g) represent the genes that participate in the nitrogen fixation mechanism, such as ferrous iron transport, translational initiation, nitrogen fixing activity and nitrogen regulatory protein. Panels (h)-(j) show the genes that take part in RNA polymerase sigma factors, cyanophycin and phycobilisomes degradation. Panels (k)-(n) represent the genes that are involved in biogenesis of ribosomes and RNA metabolism, such as ribosomal proteins, poly(A) polymerase and RNA helicase. See legend to Fig 4 for other details.

doi:10.1371/journal.pone.0125148.g005

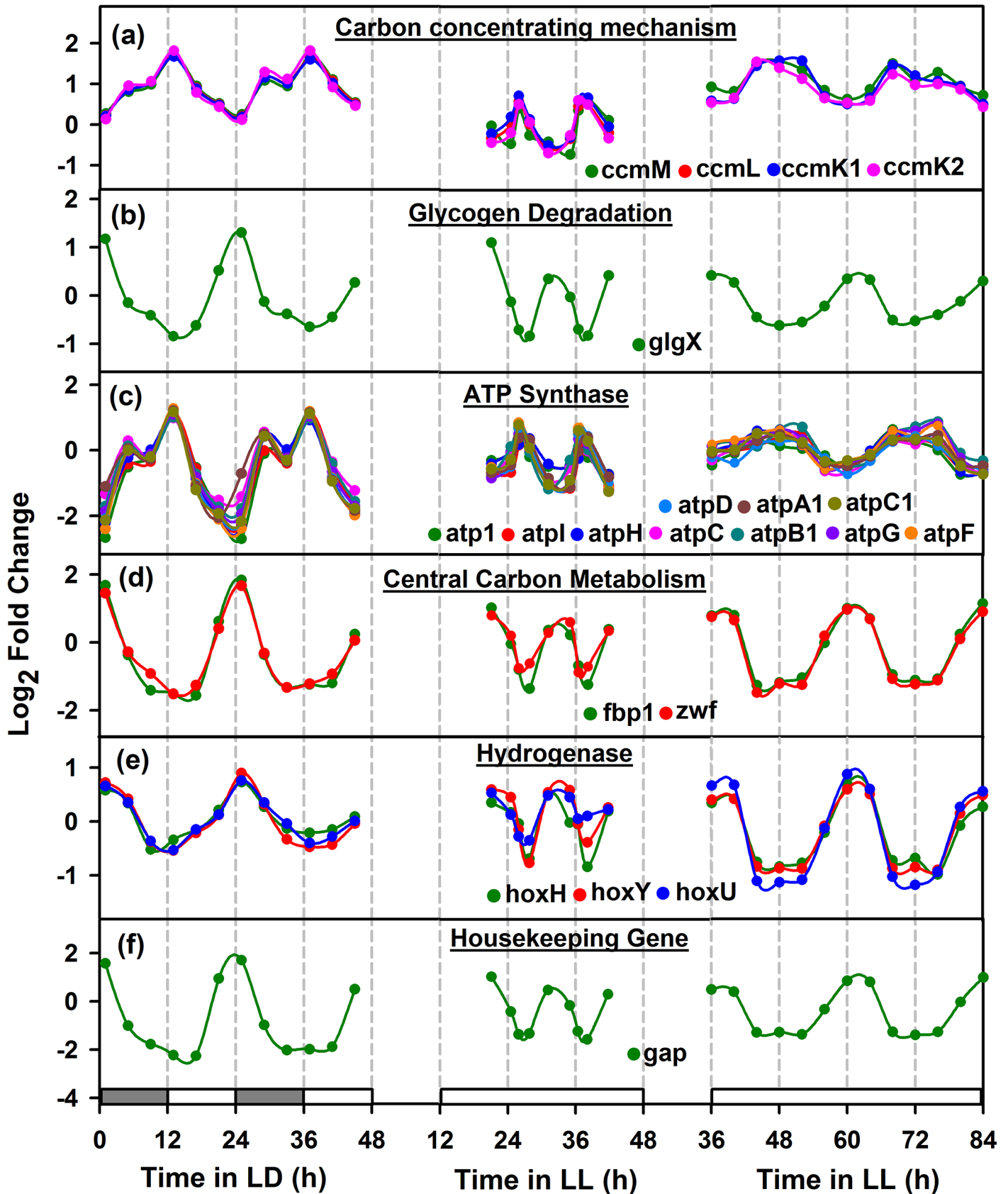


Fig 6. Comparison of oscillatory behavior of cyclic genes in nitrogen fixing (*Cyanotheca* 51142) and non-nitrogen fixing organism (*Synechococcus* 8942). Cyclic genes were selected for *Cyanotheca* 51142 and their homologs in non-nitrogen fixing *Synechococcus* 7942 (data from [32]). Panels (a) and (b) show the genes that are involved in day metabolism, such as carbon concentrating mechanism (CCM) and ATP synthase complex, peaking in the dawn or at the onset of photosynthetic phase. Panels (c)-(f) show the genes that peak during night metabolism, such as glycogen degradation, central carbon metabolism, hydrogenase and housekeeping gene, all peaking at dusk or at the onset of respiration phase or at subjective night. See legend to Fig 4 for details.

doi:10.1371/journal.pone.0125148.g006

overlapping with *nif* genes under LL. Interestingly, these genes peak around the middle of the dark phase under LD cycles, unlike the *nif* gene cluster which peak at the onset of the dark phase under LD [19]. This could be indicative that under ultradian rhythm, the resolution of the gene expression pattern might be less resolved as compared to that in the circadian rhythm under LD.

Dusk Peaking Genes

To analyze genes that peak during dusk/respiration phase, we plotted the representative genes that show oscillatory behaviour under LD and LL conditions (Fig 5). Interestingly, we noted that the genes such as NADH dehydrogenase; NADH quinone reductase; terminal oxidase; RNA polymerase sigma factor; translational initiation factor (*infB*) and nitrogen regulatory protein P-11 (*glnB*), showed peaking during early respiration (time points 1 and 5) (Fig 5(A–5C), 5(E), 5(G) and 5(H)). However, ferrous iron transport and nitrogen fixing genes showed peaking at mid or late respiration (time points 2 and 6) (Fig 5(D) and 5(F)). Furthermore, the cyanophycin genes peaked concomitantly with the nitrogenase activity (Fig 5(I)), thereby serving as a key nitrogen reserve for the organism [40]. We also noticed that the phycobilisome degradation gene (*nbla1*), up-regulating during respiration phase (time points 2 and 6) (Fig 5(J)), to control photosynthetic activity during nitrogen fixation [41,42].

Ribosome biogenesis at midnight

RNA processing (DEAD box RNA helicase). DEAD box RNA helicases are widespread in all kingdoms of life and are known to be cold-induced in some prokaryotes. They are

Table 2. Assessment of overrepresentation of Gene Ontology terms among the gene clusters of *Cyanotheca* 51142^a.

Cluster	Number of genes	Overrepresented Gene Ontology term ^b	Corrected p-value
5	55	Photosynthesis	2.70E-35
6	80	NAD(P) transhydrogenase activity	9.67E-04
7	54	Regulation of cell morphogenesis	2.97E-03
15	9	Inorganic phosphate transmembrane transporter activity	7.19E-08
23	78	Photosystem I	9.08E-09
24	80	Nitrogen fixation	8.64E-23
27	30	Electron transport chain	1.19E-03
28	62	rRNA binding	5.41E-34
29	53	Acetyl-CoA carboxylase complex	6.98E-04
30	60	Copper-transporting ATPase activity	3.53E-05
31	68	Plasma membrane proton-transporting ATP synthase complex	7.04E-13
37	64	NADH dehydrogenase (ubiquinone) activity	1.13E-08

^aGenes were clustered using the K-means algorithms. Genes of *Cyanotheca* 51142 that satisfy the 1.5-fold change filter in the gene expression data under LL (9 time points) (present study) and LD (12 time points) (data from [19]) were subjected to K-means clustering using K = 40 clusters.

^bOverrepresentation of Gene Ontology terms was performed using Biological Networks Gene Ontology tool (BiNGO) [34].

doi:10.1371/journal.pone.0125148.t002

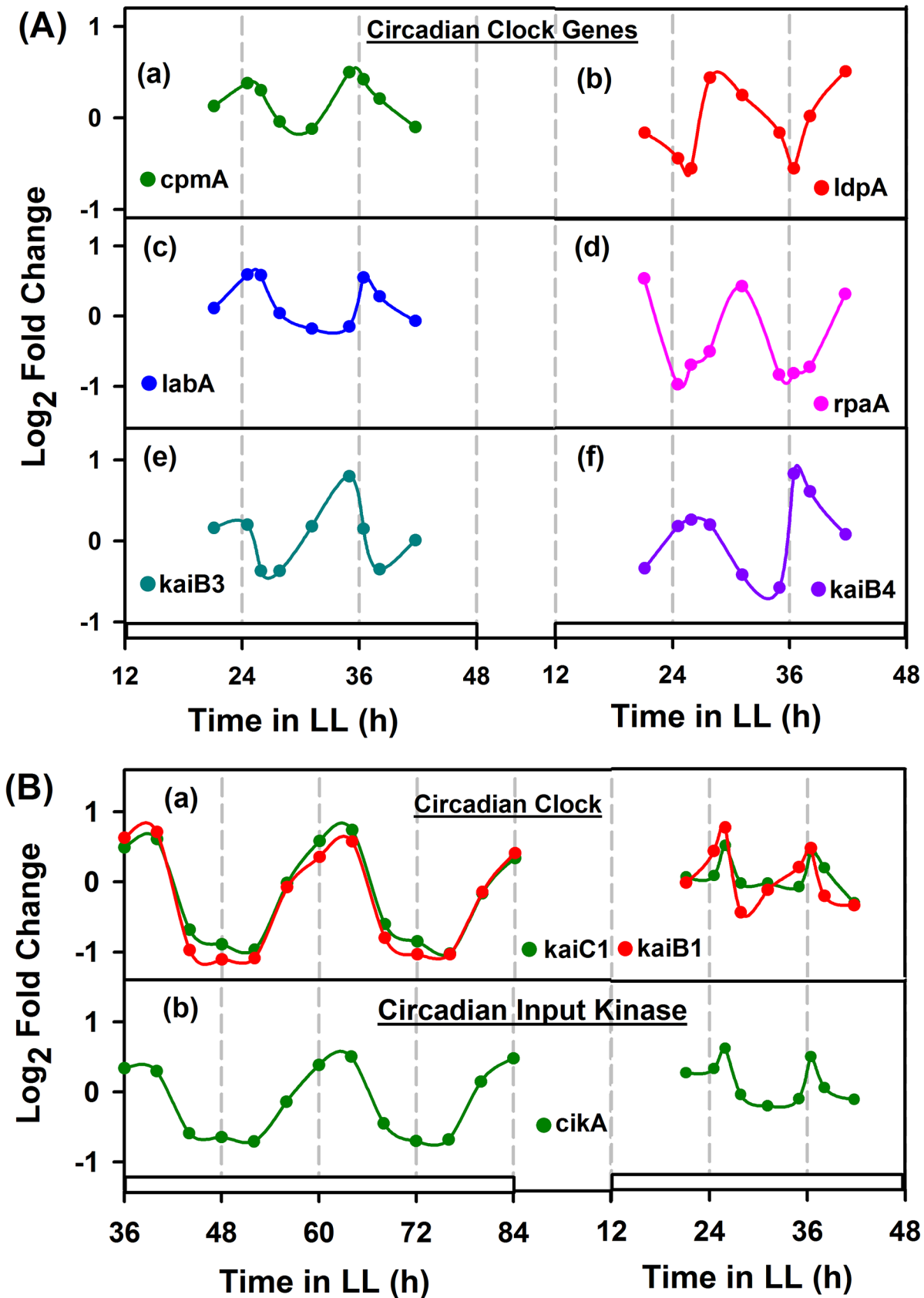


Fig 7. Oscillation in circadian clock genes. Selection of clock genes in *Cyanotheca* 51142 was performed by considering the homologues of *Synechococcus* 7942. A: Panel (a-f) shows the oscillation of clock genes in *Cyanotheca*51142 under continuous light (LL), involving in input pathway (*ldpA*), output pathway (*cpmA*, *labA*), master clock regulator (*rpaA*) and core structural clock mechanism (*kaiB3* and *kaiB4*). B: Panel (a) and (b) shows the comparison of clock genes involved in core structural clock mechanism (*kaiC1* and *kaiB1*) and input pathway of clock (*cikA*), showing 24h periodicity for *Synechococcus* 7942 and approximately 11 h periodicity for *Cyanotheca* 51142 under continuous light. White filled boxes in the X-axis, indicate the culture growth under LL condition.

doi:10.1371/journal.pone.0125148.g007

implicated in varied functions including rearrangement of RNA secondary structure that are stabilized especially at low temperatures, Ribosome biogenesis [43], and RNA turnover [44]. Deletion of the gene in *Synechocystis* shows deleterious effects at all temperatures but more prominent effects are seen at low temperatures [45]. In *Synechocystis*, the *crhR* gene has been further shown to be regulated by the redox status of the electron transport chain. The electron carrier redox state was initiated by either photosynthetic light harvesting or glucose metabolism. Interestingly, *Cyanotheca* contains *cce_4436* (*deaD*), a close homolog of *crhR*, which oscillates in LD as well as in LL. Under both conditions, the *deaD* gene peaks concomitantly with the ribosomal proteins (Fig 5N). This peak occurs at midnight under LD or during respiratory burst under LL. This first of all suggests that the gene is not merely light responsive but may be responsive to the metabolic phase or redox state. Secondly, the correlation with ribosomal proteins strongly suggests a role of *deaD* gene in ribosome biogenesis.

Light / Phase sensitive Sigma Factors / *lrtA*. It has been shown that some of the sigma factors are light activated while some others are light repressed in *Synechocystis* sp. PCC 6803 [46],[47]. For example, SigE is light induced and dark repressed while SigD is light induced. SigB is light repressed and dark induced. Other sigma factors were not found to be responsive to light. In *Cyanotheca*, we find a number of sigma factors to oscillate under LD as well as LL conditions (Figs 4 and 5). We observe that *sigD* and *sigE* to be upregulated by the end of the light phase in LD or toward the end of photosynthetic phase in LL. Likewise, *sigA* and *sigH* peak at dusk *sigC*, *sigF*, *sigG*, *sigJ* peak at dawn while *sigB* peaks at midday. In *Synechocystis* sp. PCC 6803, *sigB* is known to be heat shock inducible [47]. However, in *Cyanotheca*, we find *sigB* to oscillate both in LD and LL with peaking at mid-day or during photosynthetic phase. This first of all suggests that the sigma factors are not merely responding to light (or dark) or heat shock but also to changes in the metabolic phase of the culture. Interestingly the peaks in expression of the clock genes is followed by peaks for sigma factors such as *sigA*, *sigB*, *sigE* and *sigJ*, indicating that these sigma factors may be taking input from the clock proteins and reiterating role of circadian clock in global gene expression regulation in cyanobacteria. Although our sampling frequency does not allow us to identify precise phase behaviour of the various sigma factors, the results suggest that the sigma factors respond to the metabolic phase of the culture and may be either controlled by the energy, carbon and nitrogen status of the cell directly or through intermediaries such as the circadian clock. The light repressed protein *lrtA* has been shown to be down-regulated in response to white light in *Synechocystis* 6803 [47] and *Synechococcus* 7002 [48]. However, we find that the *lrtA* transcript oscillates in LD and LL and gets upregulated in light or under photosynthetic phase and peaks at dusk.

Programmed RNA degradation at dusk. RNA degradation used to be considered as a nuisance in laboratory protocols until two decades ago. It is now emerging that RNA degradation is programmed and is catalyzed by elaborate machinery involving a degradosome. We find a number of genes involved in RNA degradation to peak at dusk. For example, the poly(A) polymerase involved in RNA degradation peaks at dusk or relative dusk under LL (Fig 6M). This raises a question whether this suggests expedited RNA degradation at dusk, possibly for a midnight ribosome biogenesis or to shut off all the daytime enzymes. Further, we also notice

that the genes that peak at dusk or early dark do see a short half-life compared to those that peak at mid-night or at dawn.

Comparison of *Cyanothece* 51142 diurnal metabolism with *Synechococcus* 7942

To demonstrate the diurnal metabolism under continuous light, we analyzed the transcriptomic data for the present study with *Cyanothece* 51142 [19] and *Synechococcus* 7942 [32] under LD and LL conditions, respectively. We considered only the genes that show oscillation, such as from carbon concentrating mechanism, glycogen degradation, ATP synthase complex, central carbon metabolism, hydrogenase and housekeeping gene (Fig 6). Interestingly, we noticed *Cyanothece* 51142 and *Synechococcus* 7942 under respective LD and LL conditions showed ~24h periodicity, while the present study (LL) reported ~11h periodicity. Genes involved in carbon concentrating mechanism (CCM) (i.e., *ccmM*, *ccmL*, *ccmK1* and *ccmK2*) and the core genes of ATP synthesis complex (i.e., *atp1*, *atpI*, *atpH*, *atpC*, *atpB1*, *atpG*, *atpF*, *atpD*, *atpA1* and *atpC1*), showed peaking at dawn or subjective dawn (Fig 6(A) and 6(B)).

On the contrary, at night metabolism, the genes from glycogen degradation (*glgX*), central carbon metabolism (*fbp1* and *zwf*) and hydrogenase complex (*hoxH*, *hoxY* and *hoxU*) (Fig 6(B) and 6D–6E), reported peaking at early dusk or subjective dusk. Of these, *glgX* indicated the carbohydrate degradation activity to assist nitrogen fixation; genes *fbp1* and *zwf* represented the induced activity of oxidative pentose phosphate cycle under dark anoxic condition and hydrogenase complex genes suggested the characteristic reduction of protons to produce hydrogen under dark fermentative condition. Furthermore, we analyzed the housekeeping gene glyceraldehyde 3-phosphate dehydrogenase (*gap*), an internal control gene which is commonly used in the experiment [49], showed a strong expression at dusk (Fig 6(F)) suggesting that organism undergoes a controlled temporal separation of day/night cell activities in continuous light.

The clock genes and the input and output pathways

In cyanobacterial species, *Synechococcus* 7942 was the first model organism reported to have an established circadian clock mechanism. To elucidate the circadian clock behavior in *Cyanothece* 51142 under LL condition, we analyzed the transcriptomic data of central core oscillator genes (*kaiA*, *kaiB* and *kaiC*) and homologues of *Synechococcus* 7942 (*cikA*, *cpmA*, *ldpA*, *labA* and *rpaA*) that are majorly involved in input/output pathway of circadian clock system (Fig 7A and 7B). We considered only the genes that show 1.5-fold change in the expression level for the analysis.

In *Synechococcus* 7942, it has been reported that most of the genes show circadian expression at subjective dusk under continuous light [8]. However, in case of *Cyanothece* 51142, we had observed that the corresponding *kai* genes homologues oscillate in an inverse pattern to that in *Synechococcus* 7942 [18]. In the present study, we noticed similar type of induced expression for *kai* genes (*kaiC1*, *kaiB1* and *kaiB4*) during the day for *Cyanothece* 51142 (7B(a) and 7A(f)) and up-regulation in the subjective night for the genes *kaiC1* and *kaiB1* in *Synechococcus* 7942 (Fig 7B(a)) under LL condition. Interestingly, we also observed *kaiC1* plays a dominant role in the circadian clock in *Cyanothece* 51142 under our experimental conditions, as *kaiC2* does not exhibit similar oscillations (data not shown) under the culturing conditions used for the present study.

On analyzing the homolog *cikA* (*cce_4751*), an essential input pathway component for cell division, circadian phase resetting and circadian period regulation [50], showed up-regulation in the early dawn for *Cyanothece* 51142 and at subjective dusk in *Synechococcus* 7942 (Fig 7B(b)). Another *Synechococcus* homolog *ldpA* (*cce_2350*), a 'light-dependent period A' input

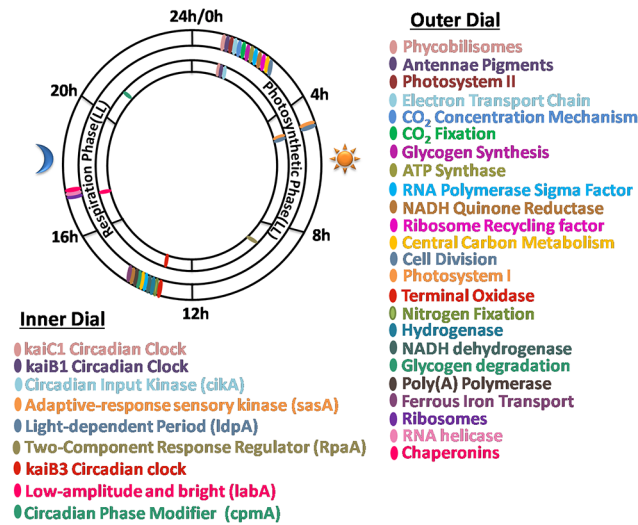


Fig 8. Peaking behavior of *Cyanotheca* 51142 genes under diurnal cycles (LD) and continuous light (LL). Clock dial shows the cellular events that peak at a particular metabolic phase under LL or at a particular time of the day under LD. Cellular events or broad cellular functions are marked on the dial if majority of genes associated with it peak at the same time or at the same phase, under LD and LL, respectively.

doi:10.1371/journal.pone.0125148.g008

clock gene, reported high expression in the late photosynthetic phase (Fig 7A(b)), suggested that it may act as ‘periodosome’ in adjusting the circadian period length according to the light intensity. It has been also reported that the *ldpA* gene in *Synechococcus* 7942, functions as ‘periodosome’ by modulating the circadian periodicity of length, either as ‘short period’ at high light or ‘long period’ under low light conditions [51].

We also noticed that the sensory histidine kinase gene (*sasA*), a positive input pathway regulator of circadian gene expression showed arrhythmic oscillation (data not shown), possibly due to some artifacts during sample processing or transcriptomic analysis or combined thereof. However, it has been shown that *sasA* oscillates along with its cognate response regulator *rpaA* under LL condition [18], suggesting that the possibility of KaiC-SasA-RpaA positive interaction pathway in mediating the output pathway of circadian clock. In supportive of this, the master clock regulator *rpaA* showed up-regulation in the late photosynthesis phase (7A(d)). We have also suggested a possible role of SasA in signaling the onset of nitrogenase gene complex expression from the synchronized expression of *nif* genes and *sasA* under LD as well as LL [18].

Interestingly, for the homolog *labA* (*cce_3317*), a negative regulator of circadian gene expression, we find up-regulation in the subjective night (7A(c)). It has been also reported that *labA* in *Synechococcus* 7942, peaks in the subjective night to regulate the auto-phosphorylation of *kaiC* through negative feedback mechanism [52]. While analyzing the homolog *cpmA* (*cce_2642*), an output pathway component of circadian clock, showed high expression at dusk (Fig 7A(a)), which suggested that it might play in regulating the phase or amplitude of the output rhythm.

Conclusions

A significant fraction of genes of *Cyanotheca* 51142 oscillate under diurnal cycles as well as continuous light. Fig 8 summarizes the peaking behavior of a representative set of genes. Given the sampling frequency, the time resolution of this analysis is 4 h under LD and 2 h under LL. A large fraction of genes peak either in the first 4 h of light or the first 4 h of dark. A few genes

peak in the middle of the day or night and hardly any of the metabolic genes peak late in the day or night. We find a strong relationship between the time of the day when genes peak under LD and the metabolic phase under which genes peak under LL. Based on the exhaust gas CO₂ and O₂ analysis, we broadly define the metabolic phases as photosynthetic phase, respiratory phase and the transition phases. The genes that peak at dawn and dusk under LD also peak at the beginning of photosynthesis and respiratory phases, respectively under LL. The ultradian rhythm in global gene expression further confirms it as the free running period for this organism in contrast to the hypothesis of such rhythm arising as an exception under specific growth conditions such as under elevated CO₂ and resulting independent of its circadian clock [17]. The present study hence puts this critical phenomenon in perspective for further understanding and applying the core regulatory mechanism(s) in this model organism towards engineering it for channelizing photosynthetic energy towards nitrogen fixation and hydrogen production.

Supporting Information

S1 Fig. Metabolic oscillations in *Cyanothece* 51142 organism. Figure shows the online measured exit gas O₂ profile for *Cyanothece* 51142, indicating 24h and 11h periodic oscillations under light-dark (LD) and continuous light(LL), respectively. Open circles with linear texts in the online profile, denotes the time points at which samples were collected from two diurnal cycles for gene expression analysis under LL condition. Boxes in white and grey filled and continuously white filled in the X-axis, indicate the culture growth conditions of LD and LL, respectively. A representative profile was considered for plotting from three replicates of the experiment.

(TIF)

S2 Fig. Oscillation in housekeeping genes. A set of housekeeping genes that reported in *Lyngbyamajuscula*[53], which show cyclic oscillations from the transcriptomic data of light/dark (LD) condition[19] and present study (LL) were selected for the analysis. Panel (a-d) shows the oscillation of housekeeping genes, involved in carbohydrate transport, chaperonins and ribosomal proteins. Grey and White filled and continuously white filled boxes in the X-axis, indicate the culture growth conditions of LD and LL, respectively.

(TIF)

S1 Table. Dataset of raw average intensity values. Average for the raw intensity values across nine samples was calculated for the present study under continuous light (LL). Sorting of the average raw intensity values was performed at higher order to list the highly expressed ORFs associated to various cellular functions.

(XLS)

S2 Table. Dataset of cyclic genes for *Cyanothece* 51142 under continuous light. Transcriptomic data from the present study (LL condition) was considered, to identify the cyclic genes that show a periodicity (T) of ± 1 h, using Sinusoidal and Fourier Transform parameter fitting model approach. A Residual Percent Energy (RPE) of 25 percent was used as a constraint in the model to select only the genes that show goodness of fit. To analyze the prediction results, in both Model1 (Sinusoidal) and Model2 (Fourier Transform), the genes that satisfy both the models, either of the models, none of the models, only Model1 and only Model2 were identified and listed with the corresponding gene expression values and gene annotation details.

(XLS)

S3 Table. Dataset of cyclic genes for *Cyanothece* 51142 under Light/Dark cycle. Transcriptional data from light/dark (LD) condition was considered, to identify the cyclic genes that show a periodicity (T) of ± 24 h, using Sinusoidal and Fourier Transform parameter fitting model approach. The genes that satisfy both the models, either of the models, none of the models, only Model1 and only Model2, were identified as similar to that of mentioned therein in [S2 Table](#). (XLS)

S4 Table. Dataset of cyclic genes for *Synechococcus* 7942 under continuous light. Transcriptional data from continuous light condition (LL) [32] was considered, to identify the cyclic genes that show a periodicity (T) of ± 24 h, using Sinusoidal and Fourier Transform parameter fitting model approach. For identification of genes that satisfy both the models, either of the models, none of the models, only Model1 and only Model2, similar methodology was adopted as mentioned therein in [S2 Table](#). (XLS)

S5 Table. Gene clusters of time-course profile expressed genes. Clusters of K = 40 were generated for *Cyanothece* 51142 by K-means method using 1.5 fold gene expression data from light/dark (LD) condition [19] and the present study (LL), which then mapped with the homologous genes from continuous light (LL) data for *Synechococcus* 7942 [32]. Homology for *Synechococcus* 7942 was performed using BLAST with an e-value cut-off of $1E-5$ against the protein sequences of *Cyanothece* 51142. BLAST score density values were additionally included as a standard measure to evaluate the correctness of identified homologues. To highlight the operonic genes in the clustered data, the operon information for *Cyanothece* 51142 from Cyano Operon database [54] was included for each group of the identified K = 40 clusters. (XLS)

S6 Table. Gene clusters of time-course profile expressed genes. Clusters of K = 30 were generated for *Cyanothece* 51142 by K-means method using 1.5 fold gene expression data from light/dark (LD) condition [19] and the present study (LL), which then mapped with the homologous genes from continuous light (LL) data for *Synechococcus* 7942 [32]. Homology for *Synechococcus* 7942 was performed using BLAST with an e-value cut-off of $1E-5$ against the protein sequences of *Cyanothece* 51142. BLAST score density values were additionally included as a standard measure to evaluate the correctness of identified homologues. To highlight the operonic genes in the clustered data, the operon information for *Cyanothece* 51142 from Cyano Operon database [54] was included for each group of the identified K = 30 clusters. (XLS)

Author Contributions

Conceived and designed the experiments: SK SBG PPW. Performed the experiments: SK SBG XVN. Analyzed the data: SK SBG XVN GAV MC PPW. Contributed reagents/materials/analysis tools: SK SBG XVN PPW. Wrote the paper: SK SBG XVN PPW.

References

1. Zhou J, Zhang H, Zhang Y, Li Y, Ma Y. Designing and creating a modularized synthetic pathway in cyanobacterium *Synechocystis* enables production of acetone from carbon dioxide. *Metab Eng.* 2012; 14: 394–400. doi: [10.1016/j.ymben.2012.03.005](https://doi.org/10.1016/j.ymben.2012.03.005) PMID: [22475865](https://pubmed.ncbi.nlm.nih.gov/22475865/)
2. Angermayr SA, Paszota M, Hellingwerf KJ. Engineering a cyanobacterial cell factory for production of lactic acid. *Appl Environ Microbiol.* 2012; 78: 7098–7106. doi: [10.1128/AEM.01587-12](https://doi.org/10.1128/AEM.01587-12) PMID: [22865063](https://pubmed.ncbi.nlm.nih.gov/22865063/)
3. Zehr JP. Nitrogen fixation by marine cyanobacteria. *Trends Microbiol.* 2011; 19: 162–173. doi: [10.1016/j.tim.2010.12.004](https://doi.org/10.1016/j.tim.2010.12.004) PMID: [21227699](https://pubmed.ncbi.nlm.nih.gov/21227699/)

4. Sherman LA, Min H, Toepel J, Pakrasi HB. Better living through cyanothece—unicellular diazotrophic cyanobacteria with highly versatile metabolic systems. *Adv Exp Med Biol.* 2010; 675: 275–290. doi: [10.1007/978-1-4419-1528-3_16](https://doi.org/10.1007/978-1-4419-1528-3_16) PMID: [20532747](https://pubmed.ncbi.nlm.nih.gov/20532747/)
5. Taniuchi Y, Yoshikawa S, Maeda S, Omata T, Ohki K. Diazotrophy under continuous light in a marine unicellular diazotrophic cyanobacterium, *Gloeotheca* sp. 68DGA. *Microbiology.* 2008; 154: 1859–1865. doi: [10.1099/mic.0.2008/018689-0](https://doi.org/10.1099/mic.0.2008/018689-0) PMID: [18599815](https://pubmed.ncbi.nlm.nih.gov/18599815/)
6. Reddy KJ, Haskell JB, Sherman DM, Sherman LA. Unicellular, aerobic nitrogen-fixing cyanobacteria of the genus *Cyanothece*. *J Bacteriol.* 1993; 175: 1284–1292. PMID: [8444791](https://pubmed.ncbi.nlm.nih.gov/8444791/)
7. Dean DR, Bolin JT, Zheng L. Nitrogenase metalloclusters: structures, organization, and synthesis. *J Bacteriol.* 1993; 175: 6737–6744. PMID: [8226614](https://pubmed.ncbi.nlm.nih.gov/8226614/)
8. Liu Y, Tsinoremas NF, Johnson CH, Lebedeva NV, Golden SS, et al. Circadian orchestration of gene expression in cyanobacteria. *Genes Dev.* 1995; 9: 1469–1478. PMID: [7601351](https://pubmed.ncbi.nlm.nih.gov/7601351/)
9. Ditty JL, Williams SB, Golden SS. A cyanobacterial circadian timing mechanism. *Annu Rev Genet.* 2003; 37: 513–543. PMID: [14616072](https://pubmed.ncbi.nlm.nih.gov/14616072/)
10. Shih PM, Wu D, Latifi A, Axen SD, Fewer DP, et al. Improving the coverage of the cyanobacterial phylum using diversity-driven genome sequencing. *Proc Natl Acad Sci U S A.* 2013; 110: 1053–1058. doi: [10.1073/pnas.1217107110](https://doi.org/10.1073/pnas.1217107110) PMID: [23277585](https://pubmed.ncbi.nlm.nih.gov/23277585/)
11. Ishiura M, Kutsuna S, Aoki S, Iwasaki H, Andersson CR, et al. Expression of a gene cluster *kaiABC* as a circadian feedback process in cyanobacteria. *Science.* 1998; 281: 1519–1523. PMID: [9727980](https://pubmed.ncbi.nlm.nih.gov/9727980/)
12. Iwasaki H, Taniguchi Y, Ishiura M, Kondo T. Physical interactions among circadian clock proteins *KaiA*, *KaiB* and *KaiC* in cyanobacteria. *EMBO J.* 1999; 18: 1137–1145. PMID: [10064581](https://pubmed.ncbi.nlm.nih.gov/10064581/)
13. Golden SS, Canales SR. Cyanobacterial circadian clocks—timing is everything. *Nat Rev Microbiol.* 2003; 1: 191–199. PMID: [15035023](https://pubmed.ncbi.nlm.nih.gov/15035023/)
14. Ivleva NB, Gao T, LiWang AC, Golden SS. Quinone sensing by the circadian input kinase of the cyanobacterial circadian clock. *Proc Natl Acad Sci U S A.* 2006; 103: 17468–17473. PMID: [17088557](https://pubmed.ncbi.nlm.nih.gov/17088557/)
15. Rust MJ, Golden SS, O'Shea EK. Light-driven changes in energy metabolism directly entrain the cyanobacterial circadian oscillator. *Science.* 2011; 331: 220–223. doi: [10.1126/science.1197243](https://doi.org/10.1126/science.1197243) PMID: [21233390](https://pubmed.ncbi.nlm.nih.gov/21233390/)
16. Kim YI, Vinyard DJ, Ananyev GM, Dismukes GC, Golden SS. Oxidized quinones signal onset of darkness directly to the cyanobacterial circadian oscillator. *Proc Natl Acad Sci U S A.* 2012; 109: 17765–17769. doi: [10.1073/pnas.1216401109](https://doi.org/10.1073/pnas.1216401109) PMID: [23071342](https://pubmed.ncbi.nlm.nih.gov/23071342/)
17. Cerveny J, Sinetova MA, Valledor L, Sherman LA, Nedbal L. Ultradian metabolic rhythm in the diazotrophic cyanobacterium *Cyanothece* sp. ATCC 51142. *Proc Natl Acad Sci U S A.* 2013; 110: 13210–13215. doi: [10.1073/pnas.1301171110](https://doi.org/10.1073/pnas.1301171110) PMID: [23878254](https://pubmed.ncbi.nlm.nih.gov/23878254/)
18. Gaudana SB, Krishnakumar S, Alagesan S, Digmurti MG, Viswanathan GA, et al. Rhythmic and sustained oscillations in metabolism and gene expression of *Cyanothece* sp. ATCC 51142 under constant light. *Front Microbiol.* 2013; 4: 374. doi: [10.3389/fmicb.2013.00374](https://doi.org/10.3389/fmicb.2013.00374) PMID: [24367360](https://pubmed.ncbi.nlm.nih.gov/24367360/)
19. Stockel J, Welsh EA, Liberton M, Kunnvakkam R, Aurora R, et al. Global transcriptomic analysis of *Cyanothece* 51142 reveals robust diurnal oscillation of central metabolic processes. *Proc Natl Acad Sci U S A.* 2008; 105: 6156–6161. doi: [10.1073/pnas.0711068105](https://doi.org/10.1073/pnas.0711068105) PMID: [18427117](https://pubmed.ncbi.nlm.nih.gov/18427117/)
20. Alagesan S, Gaudana SB, Sinha A, Wangikar PP. Metabolic flux analysis of *Cyanothece* sp. ATCC 51142 under mixotrophic conditions. *Photosynth Res.* 2013; 118: 191–198. doi: [10.1007/s11120-013-9911-5](https://doi.org/10.1007/s11120-013-9911-5) PMID: [23954952](https://pubmed.ncbi.nlm.nih.gov/23954952/)
21. Cerveny J, Nedbal L. Metabolic rhythms of the cyanobacterium *Cyanothece* sp. ATCC 51142 correlate with modeled dynamics of circadian clock. *J Biol Rhythms.* 2009; 24: 295–303. doi: [10.1177/0748730409338367](https://doi.org/10.1177/0748730409338367) PMID: [19625731](https://pubmed.ncbi.nlm.nih.gov/19625731/)
22. Krishnakumar S, Gaudana SB, Viswanathan GA, Pakrasi HB, Wangikar PP. Rhythm of carbon and nitrogen fixation in unicellular cyanobacteria under turbulent and highly aerobic conditions. *Biotechnol Bioeng.* 2013; 110: 2371–2379. doi: [10.1002/bit.24882](https://doi.org/10.1002/bit.24882) PMID: [23456695](https://pubmed.ncbi.nlm.nih.gov/23456695/)
23. Johnson CH, Stewart PL, Egli M. The cyanobacterial circadian system: from biophysics to bioevolution. *Annu Rev Biophys.* 2011; 40: 143–167. doi: [10.1146/annurev-biophys-042910-155317](https://doi.org/10.1146/annurev-biophys-042910-155317) PMID: [21332358](https://pubmed.ncbi.nlm.nih.gov/21332358/)
24. Yen U-C, Huang T-C, Yen T-C. Observation of the circadian photosynthetic rhythm in cyanobacteria with a dissolved-oxygen meter. *Plant Sci.* 2004; 166: 949–952.
25. Toepel J, Welsh E, Summerfield TC, Pakrasi HB, Sherman LA. Differential Transcriptional Analysis of the Cyanobacterium *Cyanothece* sp. Strain ATCC 51142 during Light-Dark and Continuous-Light Growth. *J Bacteriol.* 2008; 190: 3904–3913. doi: [10.1128/JB.00206-08](https://doi.org/10.1128/JB.00206-08) PMID: [18390663](https://pubmed.ncbi.nlm.nih.gov/18390663/)

26. Wang W, Ghosh BK, Pakrasi HB. Identification and modeling of genes with diurnal oscillations from microarray time series data. *IEEE/ACM Trans Comput Biol Bioinform*. 2011; 8: 108–121. doi: [10.1109/TCBB.2009.37](https://doi.org/10.1109/TCBB.2009.37) PMID: [21071801](https://pubmed.ncbi.nlm.nih.gov/21071801/)
27. de Lichtenberg U, Jensen LJ, Fausboll A, Jensen TS, Bork P, et al. Comparison of computational methods for the identification of cell cycle-regulated genes. *Bioinformatics*. 2005; 21: 1164–1171. PMID: [15513999](https://pubmed.ncbi.nlm.nih.gov/15513999/)
28. Benjamini Y, Hochberg Y. Controlling the False Discovery Rate: A Practical and Powerful Approach to Multiple Testing. *J R Statist Soc B*. 1995; 57: 289–300.
29. Elvitigala TR, Pakrasi HB, Ghosh BK. Modeling and simulation of diurnal biological processes in cyanobacteria. ACC'09: Proceedings of the 2009 conference on American Control Conference; 2009 Sep 10–12; St. Louis, MO. Piscataway: IEEE Press; 2009. p. 343–348.
30. Elvitigala T, Stöckel J, Ghosh BK, Pakrasi HB. Effect of continuous light on diurnal rhythms in *Cyanothece* sp. ATCC 51142. *BMC Genomics*. 2009; 10: 226. doi: [10.1186/1471-2164-10-226](https://doi.org/10.1186/1471-2164-10-226) PMID: [19445672](https://pubmed.ncbi.nlm.nih.gov/19445672/)
31. Jerri AJ. The Shannon sampling theorem—Its various extensions and applications: A tutorial review. *Proceedings of the IEEE*. 1977; 65: 1565–1596.
32. Vijayan V, Zuzov R, O'Shea EK. Oscillations in supercoiling drive circadian gene expression in cyanobacteria. *Proc Natl Acad Sci U S A*. 2009; 106: 22564–22568. doi: [10.1073/pnas.0912673106](https://doi.org/10.1073/pnas.0912673106) PMID: [20018699](https://pubmed.ncbi.nlm.nih.gov/20018699/)
33. Nigam A, Phale PS, Wangikar PP. Assessment of the metabolic capacity and adaptability of aromatic hydrocarbon degrading strain *Pseudomonas putida* CSV86 in aerobic chemostat culture. *Bioresour Technol*. 2012; 114: 484–491. doi: [10.1016/j.biortech.2012.03.007](https://doi.org/10.1016/j.biortech.2012.03.007) PMID: [22494573](https://pubmed.ncbi.nlm.nih.gov/22494573/)
34. Maere S, Heymans K, Kuiper M. BiNGO: a Cytoscape plugin to assess overrepresentation of gene ontology categories in biological networks. *Bioinformatics*. 2005; 21: 3448–3449. PMID: [15972284](https://pubmed.ncbi.nlm.nih.gov/15972284/)
35. Bandyopadhyay A, Elvitigala T, Welsh E, Stöckel J, Liberton M, et al. Novel metabolic attributes of the genus *cyanothece*, comprising a group of unicellular nitrogen-fixing *Cyanothece*. *MBio*. 2011; 2.
36. Liberton M, Austin JR, Berg RH, Pakrasi HB. Unique thylakoid membrane architecture of a unicellular N₂-fixing cyanobacterium revealed by electron tomography. *Plant Physiol*. 2011; 155: 1656–1666. doi: [10.1104/pp.110.165332](https://doi.org/10.1104/pp.110.165332) PMID: [21173021](https://pubmed.ncbi.nlm.nih.gov/21173021/)
37. Pena KL, Castel SE, de Araujo C, Espie GS, Kimber MS. Structural basis of the oxidative activation of the carboxysomal gamma-carbonic anhydrase, CcmM. *Proc Natl Acad Sci U S A*. 2010; 107: 2455–2460. doi: [10.1073/pnas.0910866107](https://doi.org/10.1073/pnas.0910866107) PMID: [20133749](https://pubmed.ncbi.nlm.nih.gov/20133749/)
38. Iancu CV, Ding HJ, Morris DM, Dias DP, Gonzales AD, et al. The structure of isolated *Synechococcus* strain WH8102 carboxysomes as revealed by electron cryotomography. *J Mol Biol*. 2007; 372: 764–773. PMID: [17669419](https://pubmed.ncbi.nlm.nih.gov/17669419/)
39. Lehmann R, Machne R, Georg J, Benary M, Axmann I, et al. How cyanobacteria pose new problems to old methods: challenges in microarray time series analysis. *BMC Bioinformatics*. 2013; 14: 133. doi: [10.1186/1471-2105-14-133](https://doi.org/10.1186/1471-2105-14-133) PMID: [23601192](https://pubmed.ncbi.nlm.nih.gov/23601192/)
40. Li H, Sherman DM, Bao S, Sherman LA. Pattern of cyanophycin accumulation in nitrogen-fixing and non-nitrogen-fixing cyanobacteria. *Arch Microbiol*. 2001; 176: 9–18. PMID: [11479698](https://pubmed.ncbi.nlm.nih.gov/11479698/)
41. Karradt A, Sobanski J, Mattow J, Lockau W, Baier K. NblA, a key protein of phycobilisome degradation, interacts with ClpC, a HSP100 chaperone partner of a cyanobacterial Clp protease. *J Biol Chem*. 2008; 283: 32394–32403. doi: [10.1074/jbc.M805823200](https://doi.org/10.1074/jbc.M805823200) PMID: [18818204](https://pubmed.ncbi.nlm.nih.gov/18818204/)
42. Stockel J, Elvitigala TR, Liberton M, Pakrasi HB. Carbon availability affects diurnally controlled processes and cell morphology of *Cyanothece* 51142. *PLoS ONE*. 2013; 8: e56887. doi: [10.1371/journal.pone.0056887](https://doi.org/10.1371/journal.pone.0056887) PMID: [23457634](https://pubmed.ncbi.nlm.nih.gov/23457634/)
43. Charollais J, Dreyfus M, Iost I. CsdA, a cold-shock RNA helicase from *Escherichia coli*, is involved in the biogenesis of 50S ribosomal subunit. *Nucleic Acids Res*. 2004; 32: 2751–2759. PMID: [15148362](https://pubmed.ncbi.nlm.nih.gov/15148362/)
44. Kujat SL, Owttrim GW. Redox-regulated RNA helicase expression. *Plant Physiol*. 2000; 124: 703–714. PMID: [11027719](https://pubmed.ncbi.nlm.nih.gov/11027719/)
45. Rosana AR, Ventakesh M, Chamot D, Patterson-Fortin LM, Tarassova O, et al. Inactivation of a low temperature-induced RNA helicase in *Synechocystis* sp. PCC 6803: physiological and morphological consequences. *Plant Cell Physiol*. 2012; 53: 646–658. doi: [10.1093/pcp/pcs020](https://doi.org/10.1093/pcp/pcs020) PMID: [22368073](https://pubmed.ncbi.nlm.nih.gov/22368073/)
46. Imamura S, Yoshihara S, Nakano S, Shiozaki N, Yamada A, et al. Purification, Characterization, and Gene Expression of All Sigma Factors of RNA Polymerase in a Cyanobacterium. *J Mol Biol*. 2003; 325: 857–872. PMID: [12527296](https://pubmed.ncbi.nlm.nih.gov/12527296/)
47. Imamura S, Asayama M, Takahashi H, Tanaka K, Takahashi H, et al. Antagonistic dark/light-induced SigB/SigD, group 2 sigma factors, expression through redox potential and their roles in cyanobacteria. *FEBS Lett*. 2003; 554: 357–362. PMID: [14623094](https://pubmed.ncbi.nlm.nih.gov/14623094/)

48. Samartzidou H, Widger WR. Transcriptional and posttranscriptional control of mRNA from *lrtA*, a light-repressed transcript in *Synechococcus* sp. PCC 7002. *Plant Physiol.* 1998; 117: 225–234. PMID: [9576792](#)
49. Barber RD, Harmer DW, Coleman RA, Clark BJ. GAPDH as a housekeeping gene: analysis of GAPDH mRNA expression in a panel of 72 human tissues. *Physiol Genomics.* 2005; 21: 389–395. PMID: [15769908](#)
50. Mackey SR, Choi J- S, Kitayama Y, Iwasaki H, Dong G, et al. Proteins Found in a CikA Interaction Assay Link the Circadian Clock, Metabolism, and Cell Division in *Synechococcus elongatus*. *J Bacteriol.* 2008; 190: 3738–3746. doi: [10.1128/JB.01721-07](#) PMID: [18344369](#)
51. Katayama M, Kondo T, Xiong J, Golden SS. *ltpA* Encodes an Iron-Sulfur Protein Involved in Light-Dependent Modulation of the Circadian Period in the Cyanobacterium *Synechococcus elongatus* PCC 7942. *J Bacteriol.* 2003; 185: 1415–1422. PMID: [12562813](#)
52. Taniguchi Y, Nishikawa T, Kondo T, Oyama T. Overexpression of *lala*, a paralog of *labA*, is capable of affecting both circadian gene expression and cell growth in the cyanobacterium *Synechococcus elongatus* PCC 7942. *FEBS Lett.* 2012; 586: 753–759. doi: [10.1016/j.febslet.2012.01.035](#) PMID: [22289183](#)
53. Jones AC, Monroe EA, Podell S, Hess WR, Klages S, et al. Genomic insights into the physiology and ecology of the marine filamentous cyanobacterium *Lyngbya majuscula*. *Proc Natl Acad Sci U S A.* 2011; 108: 8815–8820. doi: [10.1073/pnas.1101137108](#) PMID: [21555588](#)
54. Memon D, Singh AK, Pakrasi HB, Wangikar PP. A global analysis of adaptive evolution of operons in cyanobacteria. *Antonie Van Leeuwenhoek.* 2013; 103: 331–346. doi: [10.1007/s10482-012-9813-0](#) PMID: [22987250](#)